View metadata, citation and similar papers at core.ac.uk
brought to you by CORE
provided by UCL Discovery

Personalisation of Warfarin Therapy using Thermal Ink-Jet Printing

Parameswara Rao Vuddanda[1,2], Mustafa Alomari[1], Cornelius C Dodoo[1], Sarah J Trenfield[1], Sitaram Velaga[2], Abdul W Basit[1], Simon Gaisford[1*]

[1]*Department of Pharmaceutics, UCL School of Pharmacy, University College London, London, United Kingdom*

[2]*Pharmaceutical and Biomaterial Research Group, Department of Health Sciences, Luleå University of Technology, Luleå, Sweden*

Corresponding author:

Prof Simon Gaisford
Department of Pharmaceutics
UCL School of Pharmacy
University College London
London
Email: s.gaisford@ucl.ac.uk

Abstract

Warfarin is a widely used anticoagulant that is critical in reducing patient morbidity and mortality associated with thromboembolic disorders. However, its narrow therapeutic index and large inter-individual variability can lead to complex dosage regimes. Formulating warfarin as an orodispersible film (ODF) using thermal ink-jet (TIJ) printing could enable personalisation of therapy to simplify administration. Commercial TIJ printers are currently unsuitable for printing the milligram dosages, typically required for warfarin therapy. As such, this study aimed to modify a commercial TIJ printing system to formulate personalised warfarin ODFs containing therapeutic dosages. A TIJ printer was modified successfully with the printer functionality intact; the substrate (paper) rolling mechanism of the printer was replaced by printing onto a stationary stage. Free film substrates were composed of hydroxypropyl methylcellulose (20%w/w) and glycerol (3%w/w). The resulting ODFs were characterised for morphology, disintegration, solid-state properties and drug content. Printed film stability was assessed at 40°C/75% relative humidity for 30 days. Therapeutic warfarin doses (1.25 and 2.5 mg) were successfully printed onto the film substrates. Excellent linearity was observed between the theoretical and measured dose by changing the warfarin feed concentration (R^2 = 0.9999) and length of the print objective, i.e. the Y-value, (R^2 = 0.9998). Rapid disintegration of the ODFs was achieved. As such, this study successfully formulated personalised warfarin ODFs using a modified TIJ printer, widening the range of applications for TIJ printing to formulate narrow therapeutic index drugs.

Keywords:

Warfarin, thermal ink-jet printing, personalised medicine, orodispersible films, hydroxypropyl methylcellulose

1 Introduction

Warfarin is the primary drug of choice for long-term anticoagulation in a variety of conditions, including venous thrombosis, pulmonary embolism and atrial fibrillation (1, 2). However, its narrow therapeutic index and large inter-individual variability create a number of challenges (3). Warfarin dosages must be individualised for each patient to ensure that the anticoagulant effect is safe and effective, typically reflected in an International Normalised Ratio (INR) range of 2-3 (4). Critically, inadequate control of INR can lead to severe adverse effects; under-anticoagulation can predispose patients to thrombosis, whereas over-anticoagulation can increase the risk of bleeding (3).

Despite the importance of maintaining warfarin within the therapeutic range, around 50% of patients fail to achieve their target INR (5). Warfarin has also been listed in the top three most likely drugs to cause adverse reactions leading to hospital admissions (6). This could be partly explained by warfarin's inherently complex dosage regime and monitoring requirements. Therapeutic doses for different patients can vary widely, requiring anywhere between 4.5-77.25 mg per week (7, 8). However, commercially available warfarin tablets are manufactured in only a few fixed strengths (0.5mg, 1mg, 3mg and 5mg) (2). As such, patients are often required to take a combination of strengths, split tablets or take different dosages on alternate days. This increases the risk of patient confusion, medication errors and non-adherence, potentially leading to severe adverse effects or therapeutic failure (3, 9).

Personalised medicine has been suggested as a solution to ensure the safe and effective use of narrow therapeutic index drugs (10, 11). In the case of warfarin, tailored dosing has been estimated to prevent 85,000 serious bleeding events and save $1.1 billion each year within the United States alone (12). As such, there is a major clinical need for the development of warfarin as a formulation that permits dose flexibility and personalisation.

Advances in personalised medicines demand precise, rapid and flexible manufacturing platforms capable of printing customised dosage forms directly at the point of care. Inkjet printing, a form of 2-Dimensional (2D) printing, has received increasing attention within pharmaceuticals. The general process involves dissolving

or suspending an active pharmaceutical ingredient into a liquid carrier in order to create an 'ink'. The small 'ink' droplets (2-180 pL) are then ejected from a nozzle onto a solid substrate using either thermal (TIJ) or piezoelectric ink-jets. Both techniques have previously been used to deposit active pharmaceutical ingredients onto edible substrates (13, 14) (15-17). A thermal inkjet printer was utilised for this work.

In brief, a TIJ system is comprised of a print head on a cartridge which serves as a reservoir for the 'ink'. A current is pulsed through a resistive element in the print head, causing an internal temperature rise and subsequent vaporisation, nucleation and expansion of a bubble, which imparts sufficient energy to eject a droplet. The droplet is then precisely deposited onto a solid substrate; this has enabled inkjet printing to find numerous pharmaceutical applications. To date, this technology has been used to coat and load drug-eluting stents (18), to coat transdermal microneedles (13) and to manufacture drug-loaded microparticles (14, 19).

In the context of personalised medicines, TIJ could be used to print a variety of individualised dosages onto an edible substrate, such as orodispersible films (ODFs). This concept was demonstrated by Buanz. *et al.*, whereby a highly potent drug (salbutamol sulphate; 40μg/cm^2 per print pass) was printed onto an edible potato starch film (16). However, commercially available TIJ printers are only able to deposit very low doses (approximately a maximum of 35 μg/print cycle). As such, this technology is currently only suitable for formulating highly potent drugs (20).

This provides a challenge when attempting to formulate narrow therapeutic index drugs that typically require dosing within the milligram range, such as warfarin. Researchers have attempted to increase drug deposition via a number of approaches, for example by using multiple printing cycles (21) and higher feed concentrations (22). However, challenges surrounding non-linearity of drug deposition and crystallisation of active pharmaceutical ingredient were found. To extend the applications of TIJ, it is clear that a novel method to increase the amount of drug deposition is required.

As such, this study describes the modification of a commercial TIJ printing system to formulate customised warfarin ODFs (up to milligram dosages). The resulting ODFs were characterised and evaluated for drug content and stability.

2 Materials and Methods

2.1 Materials

Sodium warfarin was obtained from LKT Labs, UK; hydroxypropyl methylcellulose (HPMC) 6cp, i.e., Pharmacoat® 606 was obtained from Shin-Etsu, Japan; glycerol was from VWR chemicals, UK; and the fluoropolymer coated polyester film, Scotch pack release liner 1022, was from 3M Inc, US. Fast Green dye was purchased from Alfa Aesar, UK. The water used in all experiments was ultrapure water.

2.2 Printer modification and evaluating robustness

A Hewlett-Packard printer (HP 5940 Deskjet, USA, Figure 1) was used in this work. This printer was modified such that rather than the substrate (generally paper in the unmodified printer) passing through the printer's rollers during operation, printing was done onto a stage mounted underneath the cartridge print head. Briefly, the modification process involved the careful removal of some physical parts of the printer to make room for fixing a stationary stage under the cartridge print head as shown in Figure 1. Key sensors were also identified, carefully isolated so as not to damage these, and manually activated appropriately to ensure normal printer functioning.

HP 337 black cartridges were used in this work: these were modified by cutting off the top, draining the ink, and rinsing several times with deionised water until clear. The cartridge nozzles were then submerged in deionised water: ethanol solution (2:1) for 5 minutes.

An experiment to evaluate any potential inter- or intra-cartridge variations due to the modification was conducted. Three modified HP 337 black cartridges were used for this experiment. 1 mg/ml Fast Green dye solution was used as the "ink" for printing. 1 cm x 1 cm squares were printed in triplicate for each cartridge onto the clear acetate sheets. The print-outs were then carefully cut and immersed in 1 mL deionised water to dissolve the dye. The dye solutions were vortexed to ensure complete dissolution

after which high-performance liquid chromatography (HPLC) analysis was conducted.

The liquid chromatographic system used was Agilent Technologies 1200 series with quaternary pump and degasser. The column used was a Phenomenex C_{18} column (150 mm x 3.90 mm, 5 µm). A gradient system was adopted with acetonitrile HPLC grade as the organic phase and 55 mM acetate buffer (pH 5 ± 0.02) as the aqueous phase at a flow rate of 1 mL/min for 10 minutes. The gradient system consisted of 15% acetonitrile and 85% buffer for 6 minutes then 60% acetonitrile and 40% buffer for a minute after which 15% acetonitrile and 85% buffer run again for 3 minutes. An injection volume 10 µL was used with the column temperature set at 30 °C. A wavelength of 600 nm was used for detection.

2.3 Film Preparation

The placebo film gel was composed of HPMC and glycerol. Glycerol (3% w/w) was first dissolved in water at room temperature, followed by gradual addition of HPMC (20%w/w) under continuous stirring at room temperature. The resulting viscous solution (10 g) was stirred for 4 hours until a homogenous gel was formed. The gel was left to stand for 2 hours to eliminate any air bubbles trapped.

Placebo films were casted on a fluoropolymer coated polyester sheet using an automated film applicator (Coatmaster 510, Erichsen, Sweden) equipped with an adjustable coating blade. A fixed wet film thickness (1000 µm) and casting speed (5 mm/sec) were used. The casted films were dried in an oven for 40 min at 60°C (Binder, Sweden), followed by storage in a desiccator (23°C/40% relative humidity). The resulting film sheets were used as substrates for printing.

2.4 Printing of warfarin onto Films

Amounts of warfarin deposited onto a substrate can generally be varied by using different cartridge concentrations or by modifying the dimensions of the templates to be printed. In modifying the dimensions of the templates, a series of rectangles having

the same width but variations in their height were deposited onto the same unit area. This resulted in an increase in the amount of material deposited and the concept is referred to as 'Y-value'. An example of the Y-value concept is illustrated in Figure 2, where three black rectangles have the same width (0.5 cm) but Y-value (length of the print objective) changed from 0.5 cm to 1.5 cm in this scenario. Printing these templates onto a fixed area results in a linear increment in the volume of solution deposited. A variety of warfarin doses were printed on substrates, customised by changing the Y-value (1 – 7 cm). The printed films were dried at ambient conditions. Aqueous solutions of warfarin of varying concentrations (10, 40, 80, 160 and 300 mg/mL) were also printed using 1cm x 1cm templates.

2.5 Spray drying

300 mg warfarin and 900 mg HPMC were dissolved in 50 mL of water. The resultant aqueous solution was spray dried using a Buchi 190 Spray dryer (Switzerland) in an open configuration with air as the drying gas. The processing conditions were: air flow 357 $L\,h^{-1}$, aspiration rate 100% and solution feed rate 5 $mL\,min^{-1}$. The inlet temperature was fixed at 130°C for water. The outlet temperatures were in the range of 50–55°C.

2.6 Characterisation of Films

2.6.1 Drug Content Analysis

Films were dissolved in water under stirring for 1 hour (1 cm^2 in 50 mL). Solutions were filtered through a 0.45µm filter (Millex syringe-driven filter unit, Millipor Ltd., Ireland). The filtrate was analysed using the HPLC method described in Section 2.2 and detection performed at a wavelength of 214 nm.

2.6.2 Film Thickness and Disintegration

The thickness of the films (1cm^2) was measured using a digital micrometer (Cokraft®, Digital caliper, Sweden) at three points of each sample, and reported as mean ± SD. The disintegration time of the films was then evaluated by a modified Petri dish method (23). Samples (1×1 cm^2) were placed in a Petri dish containing 2 mL of water

and shaken at 60 rpm using arbitral shaker water bath at 37 ± 1 °C. The time until film disintegration or disruption was recorded.

2.6.3 Contact angle

The contact angle of the warfarin droplets on the placebo substrates (1 x 4 cm) was measured using the DSA100 drop shape analyser (KRÜSS GmbH, Hamburg, Germany). The contact angle was measured immediately after the drop was deposited onto the substrate. The behaviour of the printing solution on the substrate was captured using the video camera within the DSA100.

2.6.4 Viscosity of the warfarin ink solution

The viscosity of the warfarin ink solution range of 10 – 300 mg/ml was measured using an Anton Paar rolling ball microviscometer (Anton Paar, Graz, Austria). Samples were transferred to a glass viscometry capillary (1.6 mm diameter) containing a steel ball. Viscosity was determined as the time taken for the ball to fall 25 cm through the sample at an angle of 50, 60 and 70° to the horizontal; each automated, timed determination was performed four times. The measurements were performed at 25°C.

2.6.5 Solid state properties

Thermal analyses were performed using differential scanning calorimetry (DSC) and thermogravimetric analysis (TGA). DSC was performed using a differential scanning calorimeter (DSC Q1000, TA Instruments, USA) and each sample (>5 mg) was placed in a hermetically-sealed aluminium pan with a pinhole lid. The following heat-cool-heat cycles were performed with a nitrogen purge gas (50 mL/min): 1. The sample was heated from 25°C to 100°C at 10°C/min (to remove water content). 2. The sample was cooled from 100°C to 0°C without ramp. 3. The sample was re-heated from 0°C to 200°C at 10 °C/min above the melting temperature of warfarin. An empty pan was used as a reference and the instrument was previously calibrated for temperature and heat capacities using indium and sapphire. DSC results were analysed using Universal Analysis software (TA instruments, USA). TGA measurements were performed using a TGA instrument (TA instruments, USA). Approximately 5-8 mg of the film was heated from 25 to 150°C at 10°C/min using nitrogen as a purge gas (50 mL/min). Data collection and analysis were performed using Universal Analysis software (TA instruments, USA).

2.6.6 Attenuated Total Reflection-Fourier Transform Infrared Spectroscopy (ATR-FTIR)

Attenuated Total Reflection-Fourier Transform Infrared Spectroscopy (ATR-FTIR) was performed with a Perkin-Elmer Spectrum 100 FTIR Spectrometer using the universal diamond ATR attachment. The spectra were collected in the range of 4000-650cm^{-1} at ambient conditions using a minimum number of four scans per sample. Spectra were analysed with Spectrum Express software.

2.6.7 Surface morphology

Surface and cross-section morphology of films were captured with an FEI Inspect F50 Scanning Electron Microscope (SEM) (FEI, Hillsboro, OR, USA). Film cross-sections were immersed in liquid nitrogen; through a fracture by freezing method, clean-cut edges were ensured and plastic deformation avoided. These were then fixed on aluminium stubs by conductive carbon tape, and sputter-coated with gold (approx. 10–12 nm) in a high vacuum evaporator (108 Auto, Cressington Scientific Instruments Ltd, UK).

Polarised light microscopy (PLM) was performed using a Nikon microphoto-FXA light microscope to collect optical images with an Infinity 2 digital camera and capture application software (version 3.7.5).

2.6.8 Film Stability

To evaluate the film stability, samples of warfarin-printed films were packed in polyethylene-sealed pouches and stored in a glass desiccator (40°C/75% relative humidity) for 30 days. Drug recrystallisation, moisture content, surface morphology, drug content and disintegration time were examined on day 30.

2.7 Statistical analysis

Student t-test for two group comparisons and one-way ANOVA with Tukey's post hoc multiple comparisons were used to determine statistically significant differences (p-value<0.05).

3 Results and Discussion

The thermal ink-jet printer used in this work was the Hewlett-Packard (HP) 5940 Deskjet. The printer was modified such that rather than the substrate (paper in the unmodified printer) passing through the printer's rollers during operation, printing was done onto a stage mounted underneath the cartridge print head without the printer detecting the absence of paper. The key point with the printer modification is to identify the printer's sensors and manually activate these when needed.

The modifications to the printer mean that when printing an image, the substrate does not move vertically. Changing the volume of solution being deposited is achieved simply by changing the dimensions of the rectangular template used to initiate printing. The width of the rectangle is kept fixed and the height varied for the series of rectangles. Since the height is conventionally the y-axis, we denote this term as the 'Y-value'; with each y-value corresponding to the height of the rectangle in cm.

The modified printer maintained its functionality and an evaluation of its robustness was conducted using the relative standard deviation (RSD) values. RSD values of 2.17%, 0.25%, and 0.87% were obtained for the three cartridges (Table 1). These low values (less than 5% RSD) indicated the repeatability and precision of the printing procedure, highlighting the robust nature of the modified inkjet.

Using a modified TIJ printer platform, a variety of warfarin doses were successfully deposited onto film substrates. The amount of drug deposited was altered using two main methods; by changing the feed concentration and the Y-values.

Firstly, the concentration of warfarin within the initial feed solution was varied (10, 40, 80, 160 and 300 mg/mL) using a $1cm^2$ template. In this case, an excellent linear correlation was found between the feed solution concentration and warfarin dose deposition ($R^2 = 0.9999$) (Figure 3). Furthermore, highly precise and accurate doses of warfarin were deposited. These results indicate that the printing mechanism of TIJ (which involves rapid localised heating) was not affecting drug stability neither did the printer modification affect droplet reproducibility.

One challenge of using concentrated feed solutions is that there is a risk of drug crystallisation on the nozzle tip (and nozzle blockage), especially if the drug is at or

above saturated conditions (22). Another consideration for drop placement and accuracy is liquid viscosity (11). The viscosity of the different ink solutions of warfarin (10 – 300 mg/mL) were between 1.10 – 1.31 mPa.S, which are in line with the literature of thermal inkjet printing solutions (16).

Secondly, the Y-values (with a width of 1 cm) were varied (1-7cm) whilst maintaining a constant warfarin feed concentration (300 mg/mL). The time taken for printing of the highest length (7 cm) was 23 ± 1 sec. The correlation between Y-values and dose deposited also demonstrated good linearity, high precision and accuracy (R^2 = 0.9998) (Figure 4). At a feed concentration of 300 mg/mL and a Y-value of 7 cm, warfarin doses of 2.5 mg/cm^2 were successfully printed. However, it was observed that surface erosion and deformation of the substrate occurred at Y-values above 7 cm. This was likely due to the films being composed of a water-soluble polymer (HPMC) that may have dissolved in the aqueous environment, causing film instability and breakdown.

Encouragingly, the modified TIJ printer deposited therapeutic dosages of warfarin (2.5 mg/cm^2 using a 300 mg/mL cartridge concentration) onto substrates. This means that the physical dimensions of printed films (2×1 cm) contained warfarin doses equivalent to widely prescribed therapeutic doses (5 mg). Commercial TIJ printers are only able to deposit very low doses, making this technology currently only suitable for high potency drugs. For example, Buanz. *et al.* could print 40 µg of salbutamol sulphate onto an ODF platform (16). In this current study, by increasing the print objective Y-value, a higher amount of warfarin solution, and hence dose, was deposited. This extends the applications of TIJ printing towards formulating narrow therapeutic index drugs.

Printed films containing a 2.5 mg/cm^2 dose of warfarin were found to have a thickness of 72 ± 2 µm). No significant differences were observed when compared to the free film substrate thickness (70 ± 1 µm).

Disintegration time is considered one of the most important characteristics for the performance of ODFs. Typical disintegration times for ODFs range from 5 s to 30 s. However, there is no official method to determine disintegration of ODFs, which makes a comparison between various publications difficult. There have been many attempts at modelling *in vivo* conditions to evaluate ODF disintegration, such as the

Petri dish method and the slide frame method (25). Within this study, a modified Petri dish method was used to assess disintegration time.

In general, disintegration/dissolution of ODFs is dependent on surface tension, wettability, porosity, thickness, disintegration media and molecular interactions (26, 27). Vuddanda. *et al.* observed significant differences in the disintegration time of ondansetron ODFs that possessed different microstructures (28). Furthermore, Preis. *et al.* reported different disintegration times for films prepared with different combinations of polymers (29). In this study, warfarin-printed films containing different doses (1.25 and 2.5 mg) and the free film substrate all disintegrated within 45 seconds. These results also indicate that disintegration was not significantly affected by the presence of warfarin. The printed film disintegration times are in agreement with ODFs composed of HPMC reported in literature (30).

To determine the surface interaction between the feed solution and film substrates, the contact angle of the warfarin printing solution (300 mg/mL) was measured. Following immediate deposition on the substrate, the contact angle was 38.18 ± 1°. The deposited droplet rapidly penetrated the surface of the substrate, suggesting the warfarin was absorbed into the substrate matrix. Neither surface erosion nor dissolution of the substrate was visually observed at the printing site during contact angle analysis.

DSC thermograms of samples are shown in Figure 5. A broad endothermic peak at T_{onset} (ΔH_f) =190.6 °C was observed in the DSC thermogram of pure warfarin and physical mixture (1:3), indicating that warfarin was in the crystalline state and could be detected by DSC. Interestingly, for the TIJ printed films, no melting peak was observed, indicating that warfarin was present in the amorphous phase (31). This may be due to HPMC inhibiting the crystal growth in solid dispersions by preventing molecular mobility due to its complex polymer network (32, 33).

To further explore this, a solid dispersion of warfarin and HPMC (1:3) was prepared by spray drying. The drug content was equivalent to that of the printed films containing 2.5 mg/cm^2. DSC has been found to be an appropriate technique to determine drug solubility within a polymer (34). The characteristic warfarin recrystallisation peak was not observed in the thermogram of the spray dried solid

dispersion (**Error! Reference source not found.**), confirming that warfarin was present in the amorphous state within the HPMC polymer substrate.

Water content was analysed based on the weight loss of films using TGA. The weight loss of the warfarin-HPMC spray-dried product was 0.40%, confirming water removal during the spray drying process. For film substrates and freshly printed films, the observed weight losses were 0.86% and 1.14%, respectively (Figure 6). In the case of printed films kept under accelerated storage conditions for 30 days (40 °C/ 75% relative humidity), weight losses were higher at 3.05%. This was likely due to the higher moisture content within the storage environment.

The ATR-FTIR spectra for warfarin (pure), spray dried warfarin-HPMC and TIJ printed warfarin films (freshly printed and stability) are shown in **Error! Reference source not found.**. ATR-FTIR spectrum of pure warfarin showed the following characteristic sharp intense bands; the stretching of lactone C=O bond is observed at 1681 cm^{-1}, the asymmetric bending vibrations of CH_3 group are observed at 1451 cm^{-1} and the out-of-plane bending vibrations of C-H of phenyl rings are observed at 762 cm^{-1}. The band at 1223 cm^{-1} can be attributed to the hemiketal hydroxyl in-plane bending vibration (35). Noticeably, for warfarin-HPMC spray dried and printed films, vibrational bands with lower intensities and minor shifts of C-H of phenyl (760 cm^{-1}) and CH_3 (1451 cm-^{1}) were observed. Furthermore, bands at 1223 cm^{-1} and 1681 cm^{-1} were completely diluted or showed a lower intensity in the spray dried and printed samples. These shifts in spectral bands could be attributed to the amorphisation of warfarin and/or possible intermolecular hydrogen bonding between warfarin and HPMC. Significant spectral shifts were not observed in the case of stability tested samples compared to freshly printed films.

The surface morphologies of both the free film substrate and warfarin printed films were observed using SEM (Figure 8). Figure 8a shows the free film substrate, which exhibited an irregular and porous microstructure compared to the freshly printed film, which showed a parallel and uniform droplet-printing pattern (Figure 8b). The cross-sectional SEM images qualitatively showed the homogenous microstructure of the HPMC polymer matrix substrate. Typical drug printing impressions can be observed on top of the substrate for printed warfarin films.

Polarised light microscopy (PLM) images of substrates and printed films were in agreement with SEM images Figure 9. Neither drug crystallisation nor surface deformation was observed. Buanz. *et al.* reported similar PLM images of clonidine printed films (36).

Warfarin printed films were stored at 40°C/75% relative humidity for 30 days. Drug content and disintegration time were not affected upon storage compared to freshly printed warfarin films (Table 2). Furthermore, drug recrystallisation or erosion of films was not observed in SEM images (surface and cross-section) or PLM images. This was supported by the absence of a characteristic warfarin melting point peak (~187°C) in the endotherm of printed film, confirming warfarin was present in the amorphous phase. This may be due to warfarin being dispersed at a molecular level or adequately solubilised within the HPMC substrate. However, marked changes (buckling with partial crumbling) on the surface microstructure occurred on storage (Figure 8 and Figure 9). As such, to be used clinically, moisture absorption preventative packaging might be required to retain the film's physical appearance for patient acceptance.

4 Conclusion

Personalisation of warfarin therapy is critical to ensure patient safety and maintain therapeutic effect. This study successfully formulated warfarin ODFs in a range of therapeutic dosages (1.25mg and 2.5mg) using a modified TIJ printer. Doses were varied by changing the feed concentration and the length of the print objective (Y-value). In both cases, a linear relationship between the theoretical and measured warfarin dose was achieved, demonstrating a highly robust and accurate process. Compared to commercial TIJ printers, the modified system enabled a higher dose deposition, widening the range of applications to include formulating narrow therapeutic index drugs. This paper demonstrates the potential for TIJ printing to personalise warfarin therapy, reducing the risk of adverse effects and therapeutic failure.

Acknowledgement

Financial support for this work was provided by the Swedish Pharmaceutical Society, Sweden and University College London, UK.

References

1. Reynolds K, Valdes Jr R, Hartung B, M. L. Individualizing warfarin therapy. Personalised Medicine. 2007;4(1):11-31.
2. BNF. Warfarin Sodium 2017 [31 Jul 2017]. Available from: https://www.medicinescomplete.com/mc/bnf/current/PHP1494-warfarin-sodium.htm - PHP1494-medicinalForms.
3. Kimmel SE. Warfarin therapy: in need of improvement after all these years. Expert opinion on pharmacotherapy. 2008;9(5):677-86.
4. Crowther MA, Ginsberg JB, Kearon C, et al. A randomized trial comparing 5-mg and 10-mg warfarin loading doses. Archives of Internal Medicine. 1999;159(1):46-8.
5. Matchar DB, Samsa GP, Cohen SJ, Oddone EZ, Jurgelski AE. Improving the quality of anticoagulation of patients with atrial fibrillation in managed care organizations: results of the managing anticoagulation services trial. The American Journal of Medicine. 2002;113(1):42-51.
6. Pirmohamed M, James S, Meakin S, Green C, Scott AK, Walley TJ, et al. Adverse drug reactions as cause of admission to hospital: prospective analysis of 18 820 patients. BMJ. 2004;329(7456):15-9.
7. Hsaio J WW. Dosage patenting in personalised medicine Boston College Intellectual Property & Technology Forum2012 [31 Jul 2017]. Available from: http://bciptf.org/wp-content/uploads/2012/06/Dosage_Patenting_in_Personalised_Medicine.pdf.
8. Wadelius M, Sorlin K, Wallerman O, Karlsson J, Yue QY, Magnusson PKE, et al. Warfarin sensitivity related to CYP2C9, CYP3A5, ABCB1 (MDR1) and other factors. Pharmacogenomics J. 2003;4(1):40-8.
9. Wong W, Wilson Norton J, Wittkowsky AK. Influence of warfarin regimen type on clinical and monitoring outcomes in stable patients in an anticoagulation management services. Pharmacotherapy. 1999;19(12):1385-91.
10. Mini E, Nobili S. Pharmacogenetics: implementing personalised medicine. Clin Cases Miner Bone Metab. 2009;6(1):17-24.
11. Alomari M, Mohamed FH, Basit AW, Gaisford S. Personalised dosing: Printing a dose of one's own medicine. International Journal of Pharmaceutics. 2015;494(2):568-77.
12. McWilliam A, A; L, C. N. Healthcare savings from personalizing medicine using genetic testing: the case of warfarin 2006 [31 Jul 2017]. Available from: https://core.ac.uk/download/pdf/6665518.pdf.
13. Uddin MJ, Scoutaris N, Klepetsanis P, Chowdhry B, Prausnitz MR, Douroumis D. Inkjet printing of transdermal microneedles for the delivery of anticancer agents. International Journal of Pharmaceutics. 2015;494(2):593-602.
14. Lee BK, Yun YH, Choi JS, Choi YC, Kim JD, Cho YW. Fabrication of drug-loaded polymer microparticles with arbitrary geometries using a piezoelectric inkjet printing system. International Journal of Pharmaceutics. 2012;427(2):305-10.
15. Meléndez PA, Kane KM, Ashvar CS, Albrecht M, Smith PA. Thermal inkjet application in the preparation of oral dosage forms: Dispensing of prednisolone solutions and polymorphic characterization by solid-state spectroscopic techniques. Journal of Pharmaceutical Sciences. 2008;97(7):2619-36.
16. Buanz AB, Saunders MH, Basit AW, Gaisford S. Preparation of personalised-dose salbutamol sulphate oral films with thermal ink-jet printing. Pharmaceutical research. 2011;28(10):2386-92.
17. Vakili H, Wickstrom H, Desai D, Preis M, Sandler N. Application of a handheld NIR spectrometer in prediction of drug content in inkjet printed orodispersible formulations containing prednisolone and levothyroxine. Int J Pharm. 2017;524(1-2):414-23.
18. Tarcha PJ, Verlee D, Hui HW, Setesak J, Antohe B, Radulescu D, et al. The Application of Ink-Jet Technology for the Coating and Loading of Drug-Eluting Stents. Annals of Biomedical Engineering. 2007;35(10):1791-9.

19. Palmer D, Bamsey K, Groves R, Patil P, Jones H, McAleer L, et al. Printing particles: A high-throughput technique for the production of uniform, bioresorbable polymer microparticles and encapsulation of therapeutic peptides. Chemical Engineering Science. 2017;166:122-9.
20. Alhnan MA, Okwuosa TC, Sadia M, Wan KW, Ahmed W, Arafat B. Emergence of 3D Printed Dosage Forms: Opportunities and Challenges. Pharm Res. 2016;33(8):1817-32.
21. Genina N, Janßen EM, Breitenbach A, Breitkreutz J, Sandler N. Evaluation of different substrates for inkjet printing of rasagiline mesylate. European Journal of Pharmaceutics and Biopharmaceutics. 2013;85(3):1075-83.
22. Raijada D, Genina N, Fors D, Wisaeus E, Peltonen J, Rantanen J, et al. A Step Toward Development of Printable Dosage Forms for Poorly Soluble Drugs. Journal of Pharmaceutical Sciences. 2013;102(10):3694-704.
23. Garsuch V, Breitkreutz J. Comparative investigations on different polymers for the preparation of fast-dissolving oral films. Journal of Pharmacy and Pharmacology. 2010;62(4):539-45.
24. Sandler N, Maattanen A, Ihalainen P, Kronberg L, Meierjohann A, Viitala T, et al. Inkjet printing of drug substances and use of porous substrates-towards individualized dosing. J Pharm Sci. 2011;100(8):3386-95.
25. Irfan M, Rabel S, Bukhtar Q, Qadir MI, Jabeen F, Khan A. Orally disintegrating films: A modern expansion in drug delivery system. Saudi Pharmaceutical Journal. 2016;24(5):537-46.
26. Miller-Chou BA, Koenig JL. A review of polymer dissolution. Progress in Polymer Science. 2003;28(8):1223-70.
27. Vuddanda PR, Montenegro-Nicolini M, Morales JO, Velaga S. Effect of plasticizers on the physico-mechanical properties of pullulan based pharmaceutical oral films. European Journal of Pharmaceutical Sciences. 2017;96:290-8.
28. Vuddanda PR, Mathew AP, Velaga S. Electrospun nanofiber mats for ultrafast release of ondansetron. Reactive and Functional Polymers. 2016;99:65-72.
29. Preis M, Gronkowsky D, Grytzan D, Breitkreutz J. Comparative study on novel test systems to determine disintegration time of orodispersible films. Journal of Pharmacy and Pharmacology. 2014;66(8):1102-11.
30. Liew KB, Tan YTF, Peh KK. Characterization of Oral Disintegrating Film Containing Donepezil for Alzheimer Disease. AAPS PharmSciTech. 2012;13(1):134-42.
31. Gao D, Maurin MB. Physical chemical stability of warfarin sodium. AAPS PharmSci. 2001;3(1):18-25.
32. Ozaki S, Kushida I, Yamashita T, Hasebe T, Shirai O, Kano K. Inhibition of crystal nucleation and growth by water-soluble polymers and its impact on the supersaturation profiles of amorphous drugs. Journal of Pharmaceutical Sciences. 2013;102(7):2273-81.
33. Tajarobi F, Larsson A, Matic H, Abrahmsén-Alami S. The influence of crystallization inhibition of HPMC and HPMCAS on model substance dissolution and release in swellable matrix tablets. European Journal of Pharmaceutics and Biopharmaceutics. 2011;78(1):125-33.
34. Haddadin R, Qian F, Desikan S, Hussain M, Smith RL. Estimation of Drug Solubility in Polymers via Differential Scanning Calorimetry and Utilization of the Fox Equation. Pharmaceutical Development and Technology. 2009;14(1):19-27.
35. Parfenyuk EV, Dolinina ES. Development of Novel Warfarin-Silica Composite for Controlled Drug Release. Pharmaceutical Research. 2017;34(4):825-35.
36. Buanz ABM, Belaunde CC, Soutari N, Tuleu C, Gul MO, Gaisford S. Ink-jet printing versus solvent casting to prepare oral films: Effect on mechanical properties and physical stability. International Journal of Pharmaceutics. 2015;494(2):611-8.

Tables

Table 1: The area under curve for modified cartridges and the relative standard deviations for printed templates using fast green dye (n=3)

Cartridge	Average Area Under Curve	Standard Deviation	Relative Standard Deviation
1	232.33	5.03	2.17 %
2	232.33	0.58	0.25 %
3	239.33	2.08	0.87 %

Table 2: Stability data of freshly printed warfarin films (2.50 mg/ cm^2) and following 30 days' storage (n=3)

Parameters	Day 0	Day 30
Drug content (%)	99.82 ± 0.97	99.17 ± 1.02
Disintegration time (sec)	43± 2	47± 1
Disintegration time free film (sec)	42± 2	-

Figures

Figure 1: Image of out-of-the-box HP 5940 printer (left) and modified printer with stationary stage positioned (right)

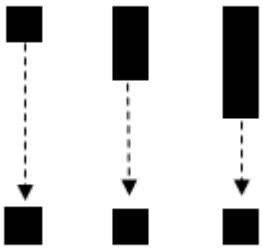

Figure 2: Illustration of the y-value concept

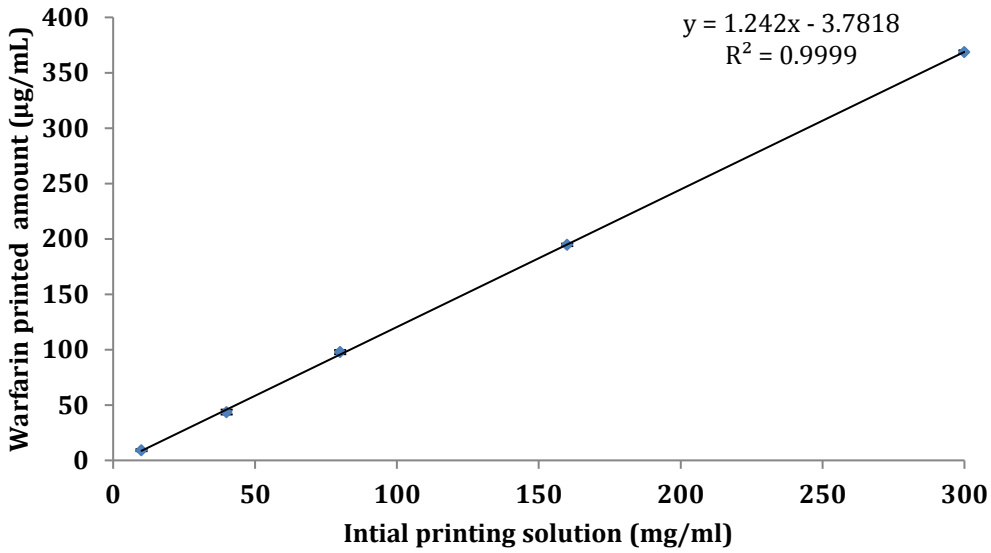

557

558 Figure 3: Amount of warfarin (µg/mL) printed onto free film substrates upon varying the feed solution
559 concentrations (mg/mL) using a 1cm^2 template (n=3).

560

561

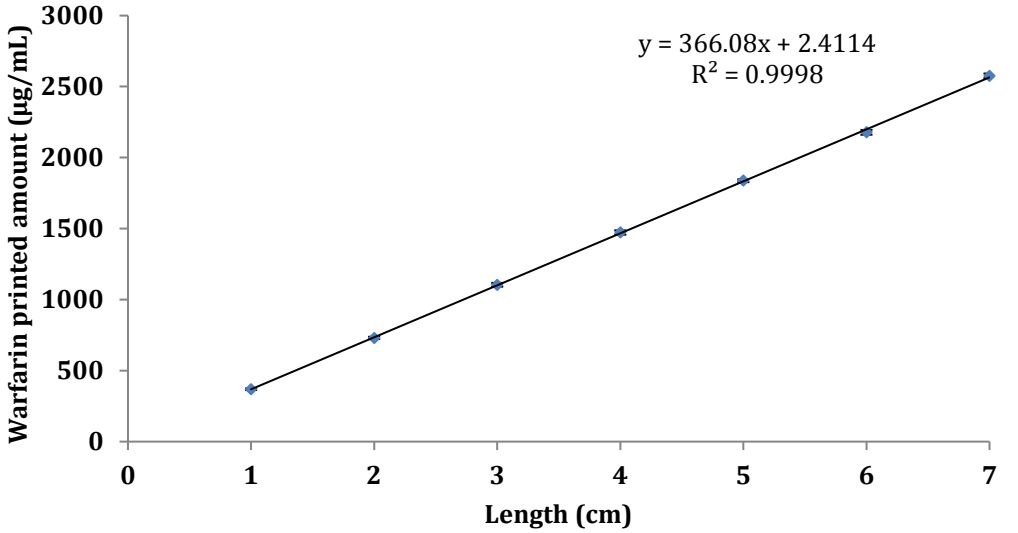

562

563 Figure 4: Amount of warfarin printed onto free film substrates upon varying Y-values at constant initial feed
564 concentration (300 mg/mL) (n=3)

565

566

567

568

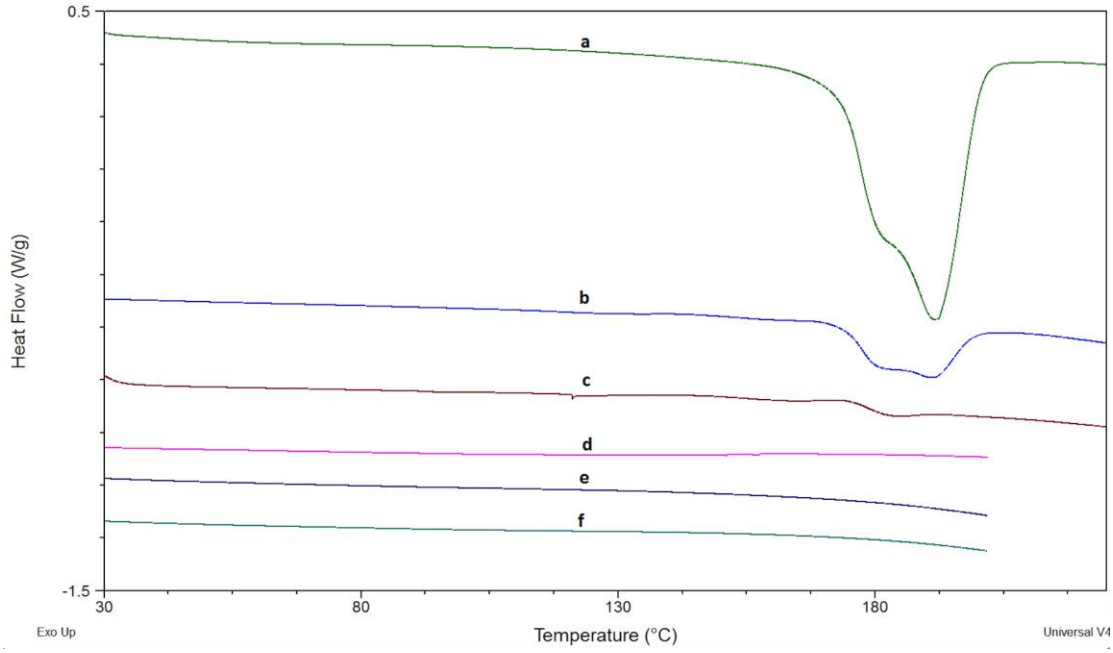

Figure 5: DSC thermograms depicting: a) warfarin (pure), b) Physical mixture of warfarin-HPMC (1:3) ratio, c) HPMC free film substrate d) Spray dried warfarin-HPMC (1:3 ratio), e) Freshly printed warfarin films, and f) warfarin printed films following 30 days' storage.

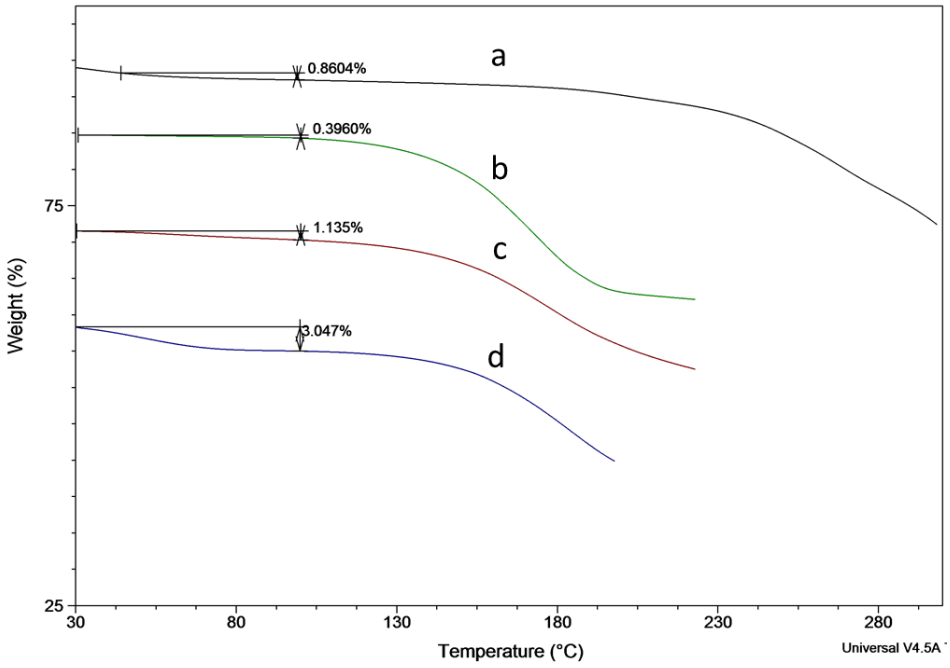

Figure 6: TGA thermograms depicting: a) HPMC free film substrate, b) Spray dried warfarin -HPMC (1:3 ratio), c) Freshly printed warfarin films and d) warfarin printed films after 30 days' storage

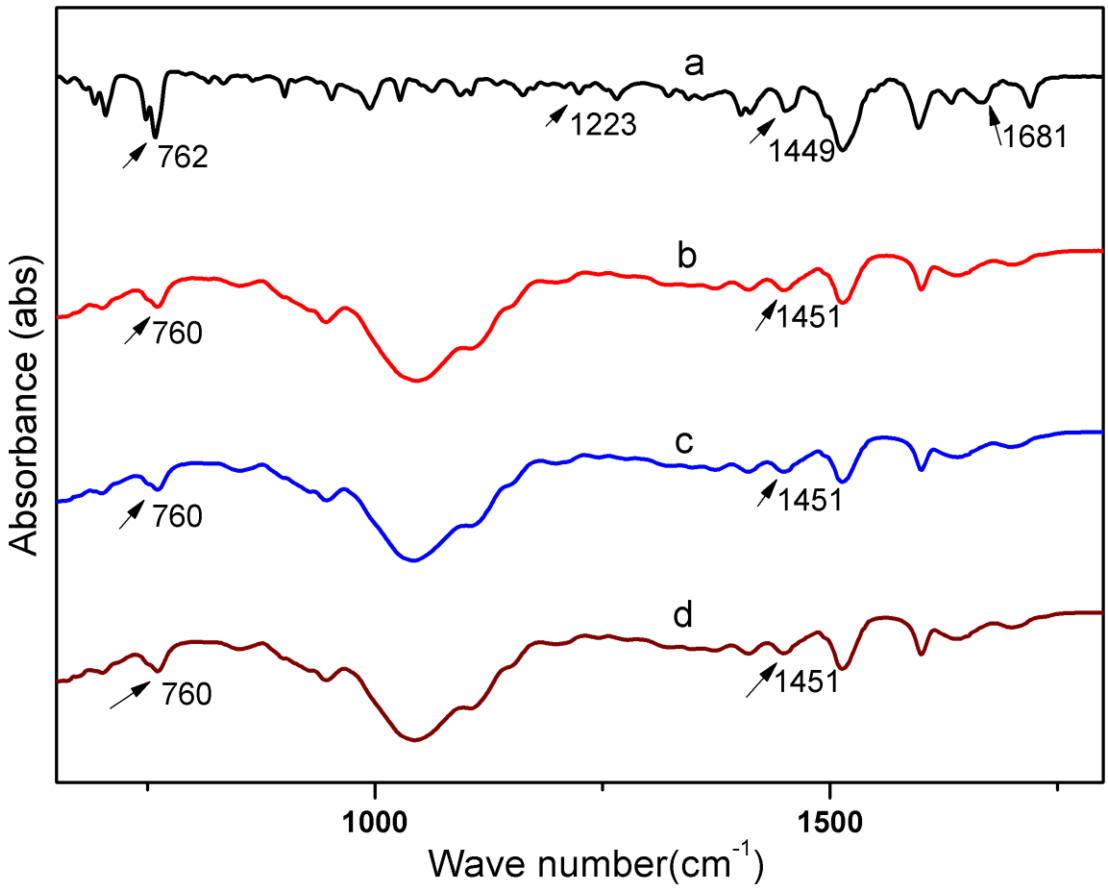

Figure 7: ATR-FTIR spectra of a) warfarin (pure), b) Spray dried warfarin-HPMC product (1:3 ratio), c) Freshly printed warfarin film and d) warfarin printed films after 30 days' storage.

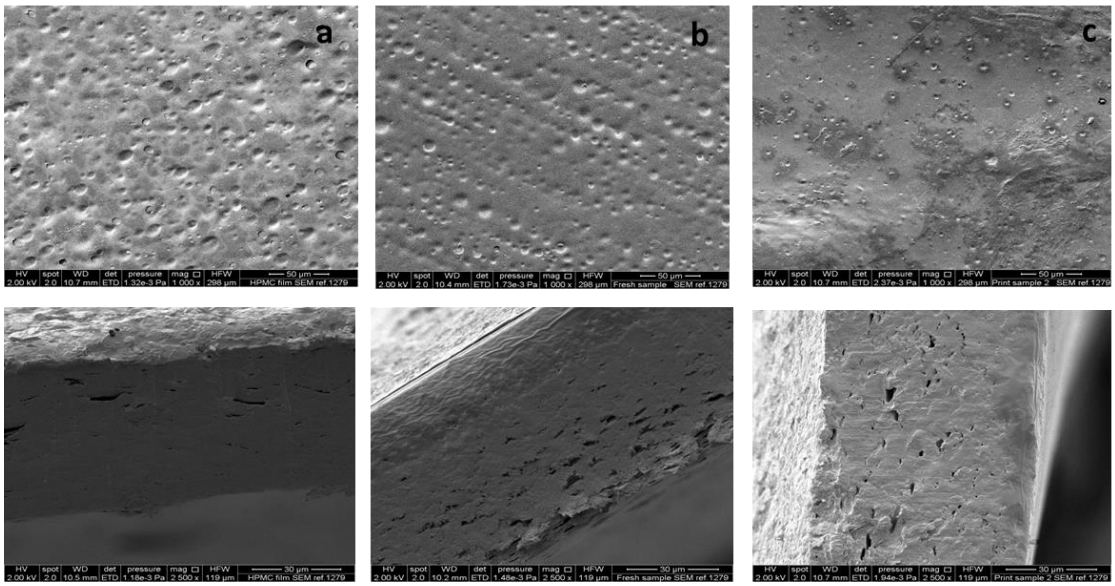

Figure 8: SEM images of a) HPMC free film substrate, b) Freshly printed warfarin films and c) warfarin printed films after 30 days' storage. Surface micrographs (top) and cross sections (bottom) of each sample set.

588 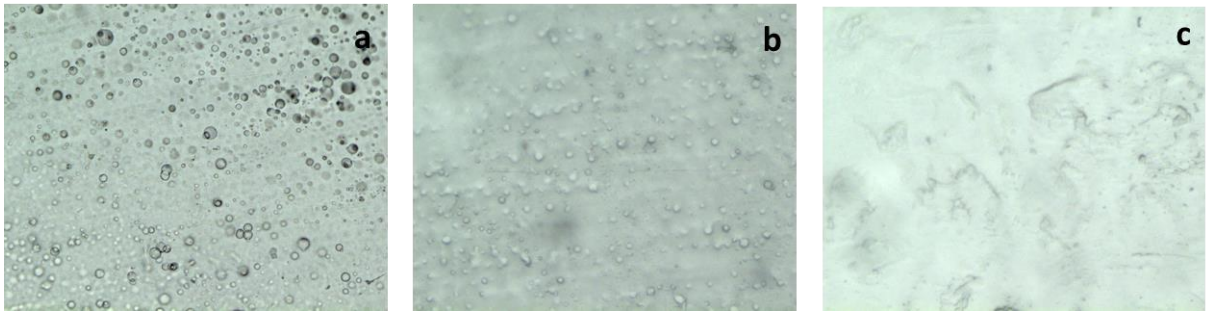

589 Figure 9: PLM images of a) HPMC free film substrates, b) Freshly printed warfarin films and c) warfarin printed
590 films after 30 days' storage.

591

592